

https://doi.org/10.1070/QEL17654

Measurement of the longitudinal relaxation time for the nitrogen nuclear spin in a nitrogen-vacancy colour centre of diamond

V.V. Soshenko, I.S. Cojocaru, S.V. Bolshedvorskii, O.R. Rubinas, A.N. Smolyaninov, V.V. Vorobyov, V.N. Sorokin, A.V. Akimov

Abstract. **A longitudinal relaxation time of a nitrogen-14 atom nuclear spin for a nitrogen-vacancy (NV) colour centre in diamond is measured by the modified double optical resonance method. The diamond sample was grown by the method of high temperature and pressure and comprised 1 ppm of NVcentres. The longitudinal relaxation time was 43(6) s, which was compared to the time calculated in the model of relaxation due to the electron spin of colour centre interaction with phonons and spin reservoir. The time measured well agrees with predictions of the model.**

Keywords: *nitrogen-vacancy colour centre, nitrogen nuclear spin.*

1. Introduction

The nitrogen-vacancy colour centre (NV centre) seems promising for using as a sensitive sensor for detecting electric and magnetic fields, pressure, and stresses [1, 2]. Later on, we will discuss the characteristic spin of an electron system in the negatively charged state (NV^-) of the colour centre, which is used in most of applications. Nitrogen included in the colour centre has a nuclear spin as well. This spin can be used in sensor applications, for example, for measuring the angular rotation rate [3–5] or as a quantum memory that improves the sensitivity of a magnetic field sensor [6]. The energy level diagram of the NV centre is presented in Fig. 1. The NV centre has an electron spin (S =1) and a nuclear spin (I = 1), with the latter being associated with nitrogen atom N^{14} (a natural concentration of this isotope is 99.6%). The ground level G splits into three electron magnetic sublevels, determined by an electron spin projection on the NV centre axis of symmetry: $|0\rangle_S$, $|\pm1\rangle_S$ (Fig. 1). The nuclear spin results in splitting each electron magnetic sublevel to three nuclear sublevels $|0\rangle_I$, $|\pm1\rangle_I$ (to the right in Fig. 1). The longitudinal relaxation time of the nuclear spin T_1 limits the information storage time while using a nuclear spin state. Depending on the sensor type, use can be made of both the time T_1 of a separate NV centre isolated from other colour centres and of the time averaged over the ensemble of NV centres. In papers [7, 8], the longitudinal relaxation time of the nuclear spin in a single NV centre measured at a field of 1.5 T was 240 s.

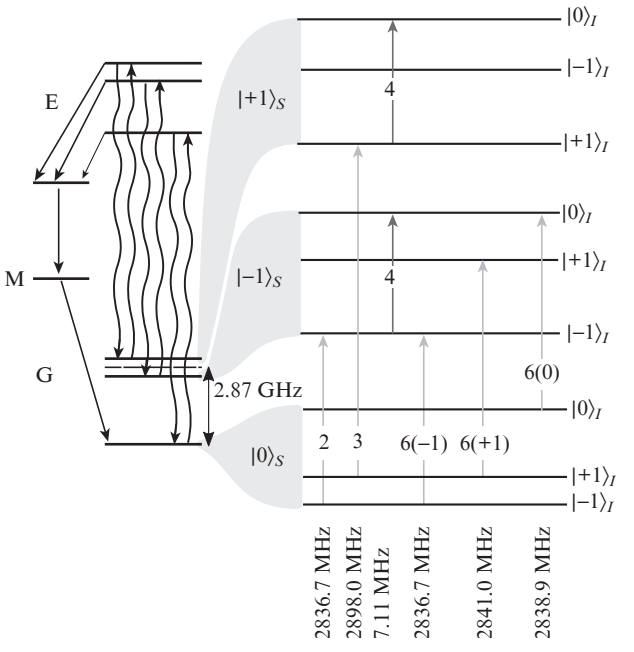

Figure 1. Energy levels of the NV centre (phonon sublevels are not shown). Wavy arrows refer to optical transitions between the ground state G and excited state E with photon emission or absorption, straight black arrows show non-radiative transitions through the metastable level M. Splitting presentation is not to scale. The structure of the ground state G is shown in the right side of the figure. When the optical radiation is switched on (excitation of the transition G → E) level G, $|0\rangle_S$ is populated due to non-radiative transitions from levels E, $|\pm1\rangle_S$ through metastable level M.

V.V. Soshenko, S.V. Bolshedvorskii, V.N. Sorokin LLC Sensor Spin Technologies, ul. Nobelya 7, Skolkovo, 121205 Moscow, Russia; Lebedev Physical Institute, Russian Academy of Sciences, Leninsky prosp. 53, 119991 Moscow, Russia; e-mail: soshenko.v@gmail.com;
I.S. Cojocaru Lebedev Physical Institute, Russian Academy of Sciences, Leninsky prosp. 53, 119991 Moscow, Russia; Russian Quantum Centre, ul. Novaya 100 A, Skolkovo, 143025 Moscow, Russia;
O.R. Rubinas LLC Sensor Spin Technologies, ul. Nobelya 7, Skolkovo, 121205 Moscow, Russia; Lebedev Physical Institute, Russian Academy of Sciences, Leninsky prosp. 53, 119991 Moscow, Russia; Russian Quantum Centre, ul. Novaya 100 A, Skolkovo, 143025 Moscow, Russia; Moscow Institute of Physics and Technology (National Research University), Institutskii per. 9, 141701 Dolgoprudnyi, Moscow region, Russia;
A.N. Smolyaninov LLC Sensor Spin Technologies, ul. Nobelya 7, Skolkovo, 121205 Moscow, Russia;
V.V. Vorobyov Universität Stuttgart, Keplerstraße 7, 70049 Stuttgart, Baden-Württemberg, Deutschland;
A.V. Akimov Texas A&M University, College Station, TX 77843, USA; LLC Sensor Spin Technologies, ul. Nobelya 7, Skolkovo, 121205 Moscow, Russia; Russian Quantum Centre, ul. Novaya 100 A, Skolkovo, 143025 Moscow, Russia

Received 22 July 2021; revision received 28 September 2021
Kvantovaya Elektronika **51** (12) 1144–1147 (2021)
Translated by N.A. Raspopov

In the present work, we report the measurement results on the longitudinal relaxation time of the nuclear spin for an ensemble of NV centres under the magnetic field of 1.1 mT sufficient for resolving the magnetic transitions and selecting one of the NV-centre orientations, because NV centres are oriented along four possible directions of covalent bonds in a diamond lattice. The electron magnetic transitions are degenerated if a magnetic field is absent. The results obtained are interesting for studying and developing sensors for magnetic field and rotation with the employment of relatively dense ensembles of NV centres.

2. Experimental setup

The experimental setup is shown in Fig. 2a. A laser diode (*1*) (WaveSpectrum WSLD-520-001-K) with a radiation wavelength of 520 nm was used. The laser radiation power was modulated by current in the switching on/off regime; the output power was 100 mW. To increase the attenuation coefficient of the laser light, the laser diode was shunted by an *n*-channel enhancement mode field-effect transistor (FET) BSS123. When the laser diode was switched off for a long time, an additional TTL-signal from a special programmable logic device (PLD) opened the FET. This technique attenuates the power of the radiation beam by more than six orders of magnitude (there was no signal from a detector with the 100-nW threshold power). The laser power was stabilised by separating part of the radiation (10%) by a beam splitter (*2*), which was detected by a photodiode (*3*) (Advanced Photonix PDB-C609-2). The laser radiation was focused by a lens (*4*) with a focal length of 50 mm to a diamond plate (*5*) onto a 6×11 μm (by 1/e intensity level) spot.

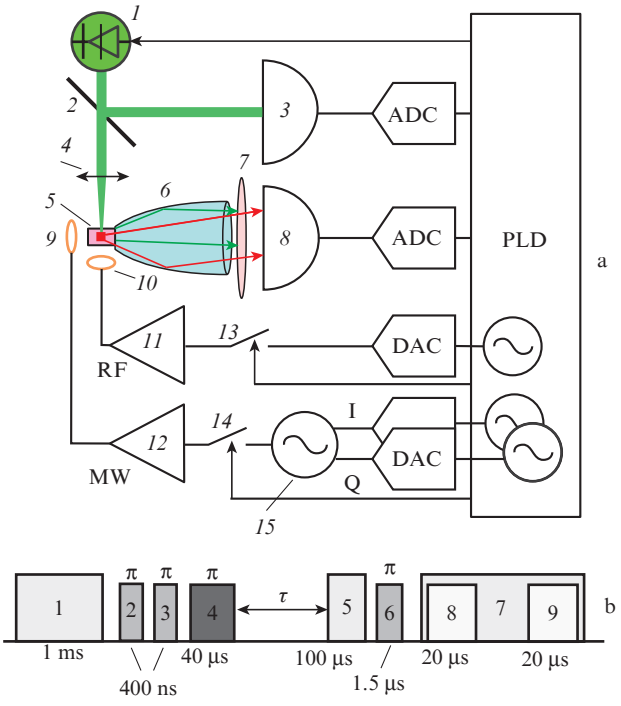

Figure 2. (a) Schematic of the experimental setup (see notations in text), and (b) experimental sequence of pulses: (1, 5, 7) laser radiation pulses; (2, 4, 6) MW and RF pulses at the frequencies of magnetic transitions (see Fig. 1); (8, 9) integration pulses for fluorescence signal.

The diamond plate measuring $1 \times 1 \times 0.6$ mm was grown by the high-pressure high-temperature method [9] (Velman LLC) and cut normally to the [111] direction. The donor nitrogen after growing was 10 ppm. NV centres were formed by subjecting the sample to irradiation and annealing. The irradiation was realised with an electron beam at the electron energy of 3 MeV; the irradiation dose was 2×10^{18} cm^{-2}. The annealing occurred at a temperature of 1400 °C. The final NV-centre concentration in diamond was about 1 ppm (1.76×10^{17} cm^{-3}); the carbon-13 concentration was natural.

Diamond fluorescence is collected by a compound parabolic concentrator (*6*) (Edmund optics CPC), passes through an optical filter (*7*) (Thorlabs LP590), which cuts off the pumping, and is detected by a photodiode (*8*) (Advanced Photonix PDB-C609-2). The photodiode signal amplified by a transimpedance amplifier was digitised by a 16-bit ADC (Analog devices AD7625) connected to the PLD (Xilinx Spartan 6). The magnetic field of 1.1 mT was produced by Helmholtz square windings with a side of 8 cm. The magnetic field induction vector was oriented along the crystallographic axis [111]. The microwave field for controlling an electron spin was formed by a resonator (*9*) described in [10]. The magnetic field in the resonator was perpendicular to the axis [111]. Microwave pulses (MW) at frequencies 2830–2900 MHz were formed by a signal generator (*15*) (SRS SG384), which was modulated in the quadrature modulation regime by a two-channel digital-to-analogue converter (DAC), which, in turn, formed an in-phase I and quadrature Q signals. A signal from the generator passed through amplifier *12* (Minicircuits ZHL-16W-43X+) to the resonator (*9*). A radiofrequency (RF) signal for controlling the nuclear spin was formed by a DAC, amplified by amplifier *11* (VectaWave VBA100-30) with an output power of 30 W and fed an antenna (*10*) realised as 20 turns of copper wire 0.2 mm in diameter (with the turn diameter of 1.5 mm). Prior to passing to the amplifiers, MW and RF signals were controlled by switches (*13*, *14*) (Minicircuits ZASWA-2-50DR+). The experiment was controlled by means of the PLD software for collecting ADC data, controlling digital frequency synthesisers, and forming the experimental sequence of pulses (Fig. 2b).

Measurements started with population of nuclear magnetic sublevel $|0\rangle_I$. Under the action of laser pulse 1 (see Fig. 2b), the electron magnetic sublevel $|0\rangle_S$ is populated. Pulses 2, 3, 4 excite magnetic transitions shown in Fig. 1 and populate the nuclear magnetic sublevel $|0\rangle_I$.

Then, the populations of nuclear sublevels relax for a time τ. Nuclear sublevel populations are measured by recording a spectrum of an optically detectable magnetic resonance (ODMR) [11]. This procedure includes a laser pre-pulse 5, a microwave π-pulse 6, and a laser pulse 7 for fluorescence recording. A signal at a single point of the ODMR spectrum is the ratio of the fluorescence signal (acquired during pulse 8) to the reference signal (acquired during pulse 9). ODMR spectra are obtained by repeating the experimental pulse sequence and varying the microwave field frequency for pulse 6. Figure 3a depicts ODMR spectra for certain values of τ. The populations of nuclear magnetic sublevels $|-1\rangle_I$, $|0\rangle_I$, and $|+1\rangle_I$ are determined from these spectra. An ODMR spectrum comprises three resonance profiles of equal widths, the amplitude of each profile being proportional to the population of the corresponding nuclear magnetic sublevel. The resonance profiles shown in Fig. 3a correspond (from left to right) to transitions 6(–1), 6(0), and 6(+1) (see Fig. 1). Populations of nuclear sublevels are determined by approxi-

mating an ODMR spectrum by the sum $S(f, S_0, C, P_{-1}, P_0, f_0, \gamma)$ of three Lorentz profiles:

$$S(f, S_0, C, P_{-1}, P_0, f_0, \gamma) = S_0 - C[P_{-1}L(f, f_0 + A_{\parallel}, \gamma) + P_0 L(f, f_0, \gamma) + (1 - P_{-1} - P_0)L(f, f_0 - A_{\parallel}, \gamma)], \quad (1)$$

$$L(f, f_0, \gamma) = \frac{\gamma^2}{(f-f_0)^2 + \gamma^2},$$

where f is the frequency of the microwave pulse 6; free parameters S_0 and C are the initial shift of the ODMR signal and sum of resonance amplitudes; f_0 is the frequency for transition 6(0); γ is the profile HWHM value; P_{-1} and P_0 are the populations of sublevels $|-1\rangle_I$, and $|0\rangle_I$, respectively; the function $L(f, f_0, \gamma)$ is the Lorentz profile of unity amplitude with the centre frequency f_0 and HWHM γ; and $A_{\parallel} = -2.14$ MHz is the value of hyperfine splitting for electron magnetic sublevels. Population P_{+1} is found by the formula:

$$P_{+1} = 1 - P_{-1} - P_0. \quad (2)$$

From ODMR spectra recorded with various time delays τ we obtained the dependence of population $P_0(\tau)$ for sublevel $|0\rangle_I$, presented in Fig. 3b. The exponential function approximates this dependence by the nonlinear least squares method:

$$P(\tau) = P_\infty + P_\delta \exp(-\tau T^{-1}). \quad (3)$$

Time T obtained in this approximation was taken at the population relaxation time for sublevel $|0\rangle_I$ and its value was 44(8) s. The random error for time T was determined from an error covariant matrix of parameters P_∞, T, and P_δ for the nonlinear least square method [12] taking into account errors of the populations obtained from an error covariant matrix for parameters S_0, C, P_{-1}, P_0, P_{+1}, f_0, and γ while approximating the ODMR spectrum. Note that at short times ($\tau < 0.1$ s) the population dependence deviates from exponential one, however, within the accuracy of 1%. Presumably, this is related to redistribution of a charge state of NV centres between neutral (NV^0) and studied (NV^-) centres. A similar behaviour was reported in [7].

The relaxation times determined by the method described above for sublevels $|-1\rangle_I$, and $|+1\rangle_I$ are, correspondingly, 40(11) and 48(18) s. By averaging the obtained relaxation times taking into account the corresponding errors, the longitudinal relaxation time of the NV-centre nuclear spin was 43(6) s.

3. Relaxation mechanism

One possible process which determines the longitudinal relaxation of a nuclear spin may be its exchange interaction with electron spin. Let us consider the Hamiltonian of the NV-centre ground state [13]:

$$H = h[D\hat{S}_z^2 + \gamma_e \boldsymbol{B}\hat{\boldsymbol{S}} - \gamma_n \boldsymbol{B}\hat{\boldsymbol{I}} + Q\hat{I}_z + A_{\parallel}\hat{S}_z\hat{I}_z + A_{\perp}(\hat{S}_x\hat{I}_x + \hat{S}_y\hat{I}_y)], \quad (4)$$

where $\hat{S}_i, \hat{I}_j$ are the operators of electron and nuclear spin projections of the ground state G onto axes i and j, respectively; $D = 2.87$ GHz is the splitting of the ground state G due to spin–spin interaction of unpaired electrons in the vicinity of

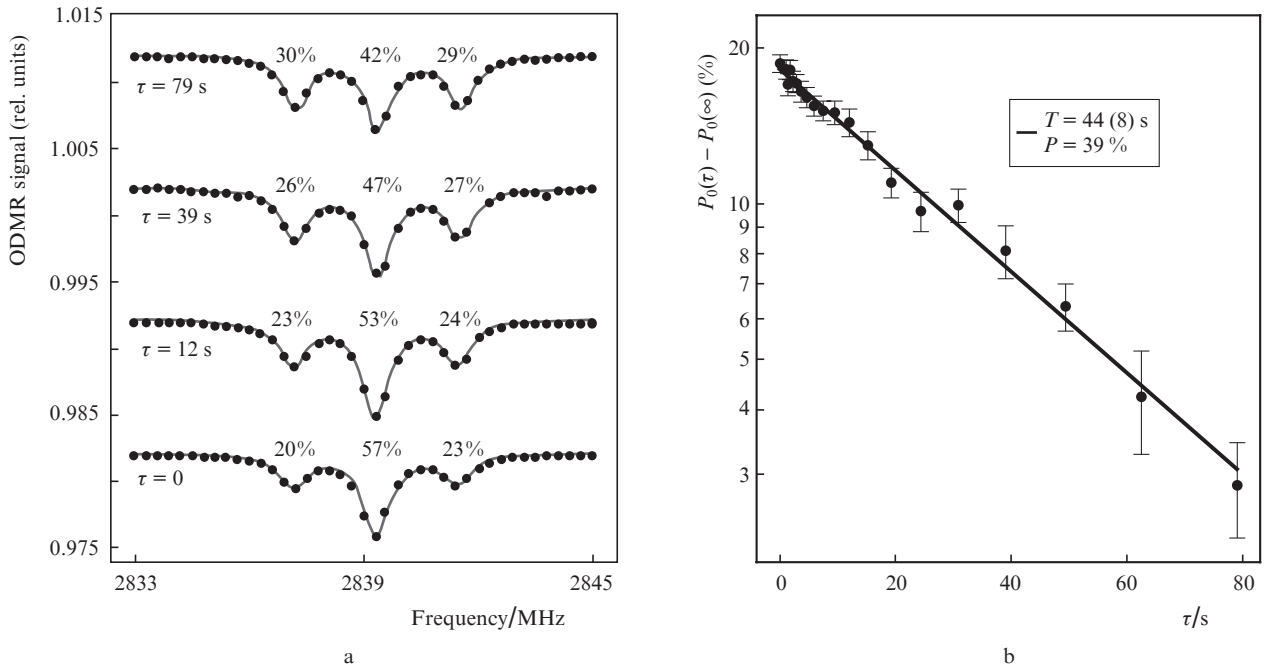

Figure 3. (a) ODMR spectra for various times τ, shifted for clearness relative each other by 0.01 along the ordinate axis (relative populations P_{-1}, P_0 and P_{+1} for sublevels $|-1\rangle_I$, $|0\rangle_I$ and $|+1\rangle_I$ are shown from left to right) and (b) dependence of the population $P_0(\tau)$ for sublevel $|0\rangle_I$ shifted by the value of population $P_0(\tau)$ at $\tau \to \infty$.

the vacancy; $\boldsymbol{B}$ is the magnetic field; $\gamma_e = 28.08$ GHz T^{-1} is the electronic gyromagnetic ratio in an NV-centre; $\gamma_n = 3.07$ MHz T^{-1} is the nuclear gyromagnetic ratio in an NV-centre; $Q = 4.95$ MHz is the quadrupole shift of nuclear sublevels; and $A_\parallel = -2.2$ MHz and $A_\perp = -2.7$ MHz are the longitudinal and transverse components for a hyperfine interaction tensor, respectively. The transverse component of the hyperfine interaction tensor $A_\perp$ is small as compared to the zero field splitting D. The basis from eigenfunctions $\hat{S}_z, \hat{I}_z$ is slightly perturbed, which leads to population exchange between nuclear and electron sublevels with an amplitude $\sim (A_\perp/D)^2$ and oscillation frequency $\sim D$. Even a weak exchange between a nuclear spin and an electron spin in the longitudinal relaxation of the latter through phonons [14] and the transverse through interaction with spin reservoir results in a relaxation of the nuclear spin.

The nuclear spin relaxation time T_{1n} was estimated in the model, in which the electron spin is related to lattice vibrations with a characteristic relaxation time $T_{1e} = 5$ ms and time of the dephasing $T_{2e} = 100$ μs caused by electron spin interaction with surrounding paramagnetic impurities. The electron spin relaxation time was measured according to the protocol described in [14], the dephasing time was found with the help of the spin echo. The time dependence of nuclear magnetic sublevel populations was found by solving numerically the Liouville equation

$$\frac{\mathrm{d}\rho}{\mathrm{d}t} = -\frac{\mathrm{i}}{h}[H,\rho] - \left\{\frac{\partial\rho}{\partial t}\right\}_{\mathrm{relax}}.$$

For the initial state we used the polarised state of the nuclear spin $\rho(0) = |0\rangle_S \otimes |0\rangle_I\langle 0|_I \otimes \langle 0|_S$. The dissipative term $\{\partial\rho/\partial t\}_{\mathrm{relax}}$ is constructed in such a way that the longitudinal relaxation rate for the electron spin is $1/T_{1e}$ and the off-diagonal elements responsible for coherence between nuclear sublevels for a single electron sublevel decay at a rate of $1/T_{2n}$; the rest off-diagonal elements decay at a rate of $1/T_{2e}$.

At such values of times T_{1e}, T_{2e}, and T_{2n}, the relaxation time for nuclear spin was 29 s. An increase in the dephasing time T_{2e} to 160 μs makes it possible to completely match the experimental and theoretical values. Thus, the most probable mechanism of nuclear spin relaxation in the considered ensembles is relaxation of the electron spin and hyperfine interaction of the nitrogen nuclear spin with the electron spin of the NV centre.

The longitudinal relaxation time of the nuclear spin for a nitrogen-vacancy colour centre in diamond measured in a weak magnetic field of 1.1 mT was 43(6) s. The experimental value well agrees with the time obtained from the relaxation model related to the electron spin interaction of the colour centre with phonons of the crystal lattice and spin reservoir.

Acknowledgements. The work was supported by the Innovation Promotion Fund (Grant No. 13156GU/2018) in the part of diamond plate preparation. In the part of measuring longitudinal relaxation of nuclear spin, the work was supported by the Russian Foundation for Basic Research (Grant No. 21-42-04407).

References

1. Schloss J.M., Barry J.F., Turner M.J., Walsworth R.L. *Phys. Rev. Appl.*, **10** (3), 034044 (2018).
2. Chen E.H., Clevenson H.A., Johnson K.A., Pham L.M., Englund D.R., Hemmer P.R., Braje D.A. *Phys. Rev. A*, **95**, 053417 (2017).
3. Ledbetter M.P., Jensen K., Fischer R., Jarmola A., Budker D. *Phys. Rev. A*, **86**, 052116 (2012).
4. Ajoy A., Bissbort U., Lukin M.D., Walsworth R.L., Cappellaro P. *Phys. Rev. X*, **5**, 011001 (2015).
5. Soshenko V.V., Bolshedvorskii S.V., Rubinas O., Sorokin V.N., Smolyaninov A.N., Vorobyov V.V., Akimov A.V. *Phys. Rev. Lett.*, **126**, 197702 (2021).
6. Jiang L., Hodges J.S., Maze J.R., Maurer P., Taylor J.M., Cory D.G., Hemmer P.R., Walsworth R.L., Yacoby A., Zibrov A.S., Lukin M.D. *Science*, **326**, 267 (2009).
7. Pfender M., Aslam N., Sumiya H., Onoda S., Neumann P., Isoya J., Meriles C.A., Wrachtrup J. *Nat. Commun.*, **8** (1) (2017). DOI: 10.1038/s41467-017-00964-z.
8. elib.uni-stuttgart.de/bitstream/11682/10198/3/diss_pfender.pdf.
9. Rubinas O.R., Vorobyov V.V., Soshenko V.V., Bolshedvorskii S.V., Sorokin V.N., Smolyaninov A.N., Vins V.G., Yelisseyev A.P., Akimov A.V. *J. Phys. Commun.*, **2**, 115003 (2018).
10. Soshenko V.V., Rubinas O.P., Vorobyov V.V., Bolshedvorskii S.V., Kapitanova P.V., Sorokin V.N., Akimov A.V. *Bull. Lebedev Phys. Inst.*, **45**, 237 (2018) [*Kr. Soobshch. Fiz. FIAN*, **45** (8), 20 (2018)].
11. Dréau A., Lesik M., Rondin L., Spinicelli P., Arcizet O., Roch J.F., Jacques V. *Phys. Rev. B*, **84**, 195204 (2011).
12. Bevington P.R., Robinson D.K., Blair J.M., Mallinckrodt A.J., McKay S. *Comput. Phys.*, **7**, 415 (1993).
13. Loubser J.H.N., van Wyk J.A. *Reports Prog. Phys.*, **41**, 1201 (1978).
14. Mrózek M., Rudnicki D., Kehayias P., Jarmola A., Budker D., Gawlik W. *EPJ Quantum Technol.*, **2**, 22 (2015).